Observation of nucleon transfer and deuteron breakup on d+^{13}C system

D. M. Janseitov[a,b,c], D. Alimov[a], D.S. Valiolda[a,b], Sh. Kazhykenov[b], B. Mauyey[c,d], K. W. Kemper[e], and Sh. Hamada[f]

[a] *Institute of Nuclear Physics, Almaty, 050032, Republic of Kazakhstan,*
[b] *Al-Farabi Kazakh National University, Almaty, 050074, Republic of Kazakhstan,*
[c] *Joint Institute for Nuclear Research, Dubna, 141980, Russian Federation,*
[d] *L.N.Gumilyov Eurasian National University, Astana, 010000, Republic of Kazakhstan,*
[e] *Department of Physics, Florida State University, Tallahassee, Florida 32306, USA.*

Received 19 September 2024; accepted 9 December 2024

The advanced computational methods continuum-discretized coupled-channel (CDCC) and coupled-reaction channel (CRC) approaches were used to analyze several sets of experimental data, including the angular distributions of ^{13}C(d,d)^{13}C at deuteron energy, E_d = 14.5 MeV, ^{13}C(d,p)^{14}C neutron stripping reaction obtained at E_d = 15.3 MeV, and data sets for ^{13}C(d,t)^{12}C neutron pickup reaction at E_d = 13.6 MeV and ^{13}C(d,n)^{14}N proton stripping reaction at E_d = 15.7 MeV. The analysis revealed that, while forward scattering angles were well described by parameter-free CDCC calculations that accounted for deuteron breakup, backward angles were significantly influenced by virtual effects from proton and neutron transfer reactions. Notably, the impacts of neutron and proton stripping reactions were substantial, reflecting their large cross sections, whereas the contribution from neutron pickup-transfer reactions was less significant.

Keywords: Deuteron breakup; transfer reaction; cluster folding model; CRC and CDCC methods.

DOI: https://doi.org/10.31349/RevMexFis.71.031204

1. Introduction

The deuteron (d), characterized by its low binding energy of 2.225 MeV, absence of bound excited states, substantial spectroscopic quadrupole moment, and propensity for dissociation into $n+p$ structure, has prompted intensive investigation into various breakup mechanisms within systems involving deuterons. The CDCC method, pioneered by Rawitscher [1] and further refined by the Kyushu group [2, 3], has catalyzed significant advancements in deuteron breakup studies. This method has emerged as a cornerstone for analyzing reactions initiated by weakly bound and halo nuclei at low energies and remains under continuous development [4]. A comprehensive analysis of deuteron elastic scattering data using the CDCC framework was conducted by Chau Huu-Tai [5]. Notably, in the case of light targets, CDCC calculations effectively reproduced deuteron elastic scattering data at forward angles, highlighting the significance of virtual breakup effects in this regime [5]. However, discernible discrepancies between predictions and experimental data at backward angles suggest the influence of couplings with alternative direct reaction pathways.

Over the years, there have been thorough examinations of transfer reactions initiated by deuterons and their influence on elastic scattering channel, with recent discoveries detailed in [6–11]. For instance, findings in Ref. [10] revealed a notable influence of the (d,p) reaction on the elastic scattering of d+^{16}O at E$_d$= 11 MeV, with a decreasing trend observed as energy increased. Furthermore, the influence of breakup diminishes as energy rises, though at a slower pace. In Ref. [8], reactions initiated by deuterons on ^{10}Be, ^{12}C, and ^{48}Ca targets across energies ranging from 12 to 71 MeV were explored, demonstrating that the elastic scattering data could be adequately reproduced by considering the coupling to deuteron breakup and the (d,p) stripping reaction. Furthermore, the authors of Ref. [7] found that the (d,^{3}He) and (d,t) reactions had a considerable effect on d+^{40}Ca elastic scattering data at E$_d$= 52 MeV, especially at scattering angles greater than 40°. In Ref. [11], deuteron breakup was found to diminish the of d+^{11}B elastic scattering differential cross section at E$_d$= 14.5 MeV, particularly at backward angles, in comparison to Optical Model (OM) results.

Contributions arising from the quadrupole moment of the deuteron ground state were found to be negligibly small relative to couplings with states from the n + p continuum. Furthermore, the influence of target excitation on the elastic scattering cross sections was similar to that of breakup effects. However, coupling to neutron-transfer reactions exhibited an opposing influence, enhancing the cross sections at backward angles to better align with experimental observations.

In this study, we analyzed various experimental datasets involving angular distributions (ADs) for ^{13}C(d,d)^{13}C elastic scattering at E_d = 14.5 MeV [12], ^{13}C(d,p)^{14}C neutron stripping reaction at E_d = 15.3 MeV [13], ^{13}C(d,t)^{12}C neutron pickup reaction at E_d = 13.6 MeV [14] and ^{13}C(d,n)^{14}N proton stripping reaction at E_d = 15.7 MeV [15]. The primary objective was to scrutinize the influence of virtual couplings with breakup and reaction processes on elastic scattering data. Methodologically, this inquiry employed the CDCC and CRC techniques for analysis, with computational implementations carried out via the code FRESCO [16]. The analysis does not directly combine the CDCC and CRC techniques, but instead relies on CRC calculations within a microscopic effective potential for the d + ^{13}C channel. This potential was derived from the CDCC calculations and thus

accounts for the projectile's breakup. The paper is structured as follows: in Sec. 2, we are discussing the effects of deuteron breakup on d+^{13}C AD at $E_d = 14.5$ MeV. Section 3 demonstrates the effects of nucleon pickup/stripping reactions on d+^{13}C AD at $E_d = 14.5$ MeV. Summary is given in Sec. 4.

2. Deuteron breakup effects on d + ^{13}C AD at 14.5 MeV

To examine the influence of deuteron breakup on the d+^{13}C elastic scattering AD at $E_d = 14.5$ MeV, we employed the CDCC method. This methodology entailed discretizing and truncating the continuum located above the deuteron breakup threshold energy, specifically at 2.225 MeV, into a sequence of momentum bins (k) of width 0.125 fm^{-1}. Utilizing a deuteron model space as delineated in Ref. [17], the computational domain extended to $k_{\max} = 0.625$ fm^{-1}, corresponding to E$_{max}$ = 16.33 MeV. Within the CDCC framework, the dynamic polarization potential (DPP) stemming from coupling to the continuum was accounted for, facilitating an examination of breakup effects. Moreover, an integral aspect of conducting CDCC computations for the d+^{13}C system involved incorporating neutron (n) and proton (p)+^{13}C potentials at suitable energies (1/2 E_d). These potentials were convoluted through a cluster folding (CF) procedure to yield the real and imaginary components of the CF potential pertinent to the d+^{13}C system, as described below:

$$V^{CF}(\mathbf{R}) = \int \left[V_{n-^{13}C}\left(\mathbf{R} - \frac{1}{2}\mathbf{r}\right) + V_{p-^{13}C}\left(\mathbf{R} + \frac{1}{2}\mathbf{r}\right) \right] |\chi_{n-p}(\mathbf{r})|^2 d\mathbf{r}, \quad (1)$$

$$W^{CF}(\mathbf{R}) = \int \left[W_{n-^{13}C}\left(\mathbf{R} - \frac{1}{2}\mathbf{r}\right) + W_{p-^{13}C}\left(\mathbf{R} + \frac{1}{2}\mathbf{r}\right) \right] |\chi_{n-p}(\mathbf{r})|^2 d\mathbf{r}. \quad (2)$$

Here ($V_{n-^{13}C}$ and $V_{p-^{13}C}$) and ($W_{n-^{13}C}$ and $W_{p-^{13}C}$) represent the real and imaginary parts of potentials for the n+^{13}C and p+^{13}C channels, sourced from the global CH89 [18] potential. Undoubtedly, the choice of the global CH89 potential is not unique; other potentials, such as those by Koning and Delaroche [19], could also be used, yielding very similar results. The n+^{13}C and p+^{13}C potentials, which were utilized in the CDCC computations, are detailed in Table I. The χ_{n-p} term represents the deuteron wave function characterizing its cluster structure [20], assumed to follow a Gaussian form as per [21], with respective parameters $V_0 = 72.15$ MeV and $r_0 = 1.484$ fm.

$$V_{n-p} = V_0 \exp - \left(\frac{r}{r_0}\right)^2. \quad (3)$$

Figure 1 illustrates the comparison between the elastic scattering AD for the d+^{13}C system at E$_d$ = 14.5 MeV and the corresponding results obtained from the CDCC calculations. The solid curve in Fig. 1 represents the results of the CDCC computations, conducted without the introduction of any adjustable parameters. Consistent with previous investigations, the CDCC calculations effectively reproduce the experimental data at forward scattering angles up to nearly 50°. However, within the 50°−100° angular range, the CDCC predictions exhibit an underestimation of the measured cross sections. By contrast, the dash-dotted curve in Fig. 1 shows the result of a one-channel calculation (1-ch CDCC) with all the breakup couplings omitted (*i.e.*, the no-coupling case). A comparison with the full CDCC results (25-chs. CDCC), reveals that deuteron breakup instigates a notable reduction in the elastic scattering cross sections at scattering angles exceeding 97°. Analogous observations of this phenomenon have been documented in other systems, such as d+^{58}Ni [22] and d+^{11}Be [23].

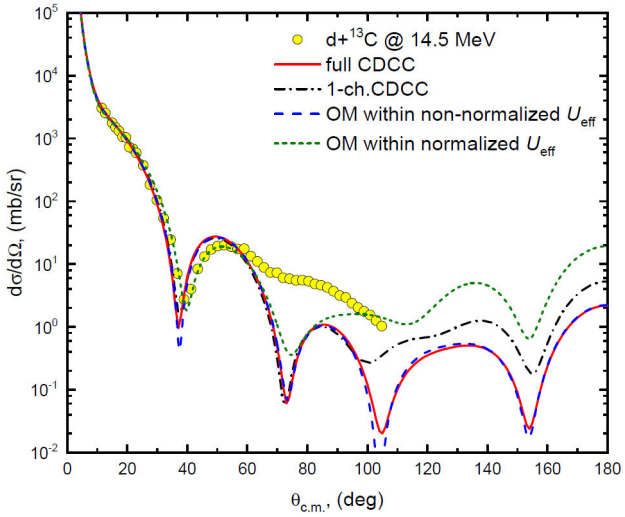

FIGURE 1. The d+^{13}C elastic AD data at $E_d = 14.5$ MeV versus and the calculations obtained through full CDCC, 1-Ch. CDCC, as well as both non-normalized and normalized U_{eff} potential.

Additionally, the d+^{13}C elastic scattering AD at $E_{lab} = 14.5$ MeV is reanalyzed using an effective potential (U_{eff}), which illustrated in Fig. 2, obtained from the microscopic CDCC calculations. The U_{eff} comprises both the CF potential (U_{CF}) and the DPP (U_{DPP}), each featured with a real component to simulate scattering and an imaginary component to simulate absorption (flux reduction), as represented in Eq. (4).

$$U_{\text{eff}}(r) = U_{CF}(r) + U_{DPP}(r), U = V + W. \quad (4)$$

As seen in Fig. 1, the result of an optical model calculation with U_{eff} as input reproduces the elastic scattering angular distribution of the full CDCC calculation very well. To improve the fit to the data, the real and imaginary parts of U_{eff} were renormalized by factors N_{Reff} and N_{Ieff}, with the optimal values being N_{Reff} = 0.914 and N_{Ieff} = 0.576, resulting in the short-dashed curve. Theses optimal values for N_{Reff} and N_{Ieff} factors were reached through minimizing the χ^2 value, that quantifies the deviation between the calculated $\sigma(\theta_i)^{cal}$ and experimental $\sigma(\theta_i)^{\exp}$ cross sections:

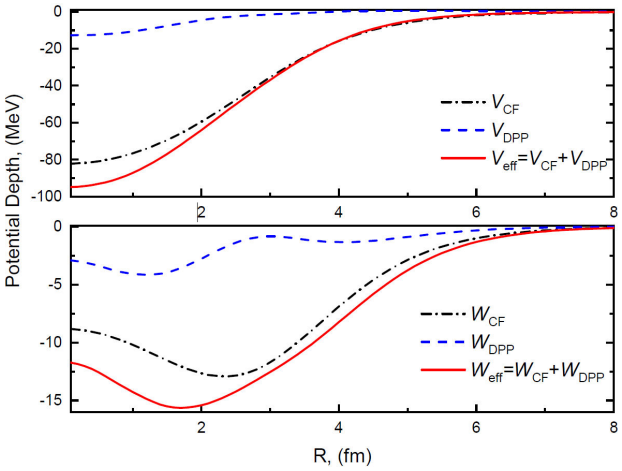

FIGURE 2. The extracted $U_{\rm eff}$ from the CDCC calculations for d+^{13}C system at E$_d$= 14.5 MeV.

$$\chi^2 = \frac{1}{N}\sum_{i=1}^{N}\left(\frac{\sigma(\theta_i)^{\rm cal}-\sigma(\theta_i)^{\rm exp}}{\Delta\sigma(\theta_i)}\right)^2, \qquad (5)$$

where $\Delta\sigma(\theta_i)$ is the relative uncertainty in experimental data. It is worth mentioning that test CDCC calculations using both the CH89 [18] and Koning and Delaroche [19] potentials produced very similar results.

3. Effects of nucleon transfer reaction on d + ^{13}C elastic scattering

3.1. ^{13}C(d,p)^{14}C neutron-stripping transfer reaction

In addition to the breakup effects, which appear at low deuterons' bombarding energies, other effects from transfer reactions could significantly influence the elastic channel cross sections. In order to investigate the probable effects of the (d,p) neutron stripping transfer reaction on the d+^{13}C elastic scattering AD, the previously measured ^{13}C(d,p)^{14}C ADs at E$_d$= 15.3 MeV leading to the (J^π= 0$^+$, 0.0 MeV), (J^π= 1$^-$, 6.09 MeV), and (J^π= 3$^-$, 6.73 MeV) ^{14}C states [13] are investigated within the framework of the CRC

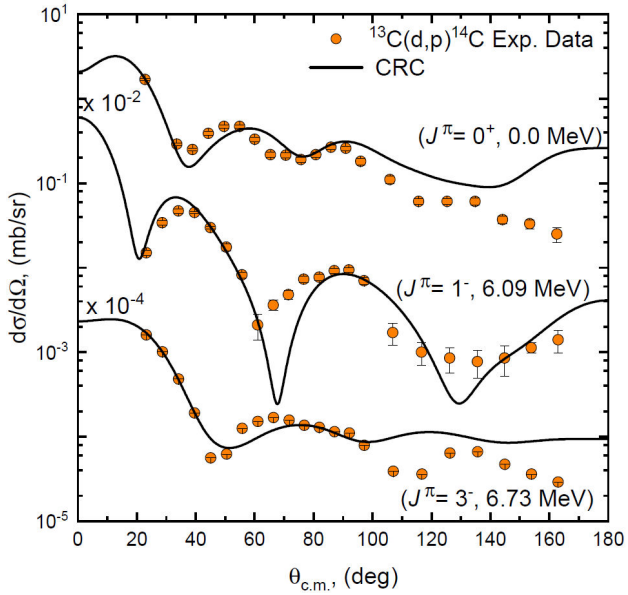

FIGURE 3. Comparison between the experimental ^{13}C(d,p)^{14}C reaction at E$_d$= 15.3 MeV [13] with the transition to the (0$^+$, 0.0 MeV), (1$^-$, 6.09 MeV), and (3$^-$, 6.73 MeV) ^{14}C states (solid circles) and the CRC calculations (solid curves).

method. The generated with the renormalization N_{Reff}= 0.914 and N_{Ieff}= 0.576 was utilized for the (d+^{13}C) entrance channel. While, for the (p+^{14}C) exit channel at appropriate energy, the CH89 potential [18] was implemented. These potentials are given in Table I. The binding potential for the following configurations: ^{14}C(0$^+$, 0.0) $\rightarrow$ ^{13}C + n, ^{14}C*(1$^-$, 6.09)$\rightarrow$ ^{13}C + n, and ^{14}C*(3$^-$, 6.73)$\rightarrow$ ^{13}C + n was taken in the usual real volume Woods-Saxon (WS) shape with a radius parameter of 1.25 fm, diffuseness of 0.65 fm, and potential depths of 43.94, 56.1, and 59.54 MeV for the three aforementioned configurations, respectively. The n + p binding potential was taken in Gaussian form, as used in the CDCC calculations. The comparison between the experimental AD for the ^{13}C(d,p)^{14}C transfer reaction leading to the aforementioned ^{14}C states at E$_d$= 15.3 MeV and the calculations within the framework of CRC method is reasonably

TABLE I. Potential parameters employed in the d+^{13}C CDCC calculations and in the CRC calculations for the ^{13}C(d,p)^{14}C, ^{13}C(d,t)^{12}C and ^{13}C(d,n)^{14}N transfer reaction.

n+^{13}C and p+^{13}C potential parameters employed in the CDCC computations												
system	V_0	r_V	a_V	W_0	r_W	a_W	W_d	r_d	a_d	V_{SO}	r_{SO}	a_{SO}
p + ^{13}C [18]	52.85	1.154	0.69	0.96	1.151	0.69	8.04	1.151	0.69	5.9	0.83	0.63
n + ^{13}C [18]	49.73	1.154	0.69	1.17	1.151	0.69	5.90	1.151	0.69	5.9	0.83	0.63
Parameters employed in the CRC computations for the ^{13}C(d,p)^{14}C reaction												
n + ^{14}C [18]	49.92	1.156	0.69	1.84	1.155	0.69	7.93	1.155	0.69	5.9	0.84	0.63
Parameters employed in the CRC computations for the ^{13}C(d,t)^{12}C reaction												
t + ^{12}C [24]	122.0	1.20	0.8				13.00	1.460	0.75	15.4	1.43	0.2
Parameters employed in the CRC computations for the ^{13}C(d,n)^{14}N reaction												
n + ^{14}N [18]	46.83	1.156	0.69	2.23	1.155	0.69	6.05	1.155	0.69	5.9	0.84	0.63

TABLE II. Spectroscopic amplitudes (SAs) employed in the CRC calculations for ^{13}C(d,p)^{14}C, ^{13}C(d,t)^{12}C and ^{13}C(d,n)^{14}N transfer reaction, asterisks means fixed values for SA from literature.

Configuration	nLj	SA (P.W.)	Previously reported values
$d \rightarrow n + p$	$1S_{1/2}$	1.0	1.0 [27]
^{14}C(0^+, 0.0 MeV)$\rightarrow$ ^{13}C+n	$1S_{1/2}$	-1.229	-1.232 [13]
			-1.094 [25]
^{14}C*(1^-, 6.09 MeV)$\rightarrow$ ^{13}C+n	$2S_{1/2}$	0.881	0.881 [13]
^{14}C*(3^-, 6.73 MeV)$\rightarrow$ ^{13}C+n	$1D_{5/2}$	0.733	0.718 [13]
			-0.994 [26]
^{3}H$\rightarrow$ $d + n$	$1S_{1/2}$	1.2247	1.2247 [27]
^{13} C $\rightarrow$^{12}C(0^+, 0.0 MeV)+n	$1P_{1/2}$	0.201	0.601 [28]
^{13}C$\rightarrow$ ^{12}C(2^+, 4.43 MeV)+n	$1P_{3/2}$	-0.524	-1.124 [29]
^{14}N$\rightarrow$ ^{13}C+p	$1P_{1/2}$	1.203	0.461 [30]
	$1P_{3/2}$	0.578	0.163 [30]

good as illustrated in Fig. 3. The Optimal SAs for the configurations ^{14}C(0^+, 0.0)$\rightarrow$ ^{13}C + n, ^{14}C*(1^-, 6.09)$\rightarrow$ ^{13}C+ n, and ^{14}C*(3^-, 6.73)$\rightarrow$ ^{13}C + n were obtained from fitting the experimental data in the full angular range through minimizing the χ^2/N, and their listed values in Table II are in a reasonable agreement with the previously reported values [13, 25, 26].

3.2. ^{13}C(d,t)^{12}C neutron-pickup transfer reaction

To examine the coupling effects of the (d,t) neutron transfer reaction on the d+^{13}C elastic scattering channel, we investigate the previously measured ADs for the ^{13}C(d,t)^{12}C transfer reaction at $E_d = 13.6$ MeV, leading to the ($J^\pi = 0^+$, 0.0 MeV) and ($J^\pi = 2^+$, 4.43 MeV) ^{12}C states [14]. This investigation is conducted within the CRC method. The key components necessary for CRC calculations include optimal potentials for both the (d+^{13}C) and (t+^{12}C) channels at suitable energies, along with the spectroscopic amplitudes (SAs) for the relevant overlaps. For the (d+^{13}C) channel, we employed the generated with renormalizations $N_{Reff} = 0.914$ and N_{Ieff}= 0.576. While the potential for the (t+^{12}C) channel was taken from Ref. [24]. In order to get a good description for the transfer to the considered ^{12}C states AD data, we had to perform a search for the optimal SA for the ^{13}C$\rightarrow$ ^{12}C(0^+, 0.0 MeV) + n and ^{13}C$\rightarrow$ ^{12}C*(2^+, 4.43 MeV) + n configurations using the SFRESCO search code [16]. The comparison between the experimental ADs for the ^{13}C(d,t)^{12}C transfer reaction at $E_d = 13.6$ MeV leading the ($J^\pi = 0^+$, 0.0 MeV) and ($J^\pi = 2^+$, 4.43 MeV) ^{12}C states and the CRC calculations using potential parameters given in Table I, is shown in Fig. 4. The SAs for the configurations ^{13}C$\rightarrow$ ^{12}C(0^+, 0.0 MeV) + n and ^{13}C$\rightarrow$ ^{12}C*(2^+, 4.43 MeV) + n were obtained from fitting the measured data at the most forward angles, and they underestimate the previously reported values [28, 29] as shown in Table II. The d + n bound-state potential was taken in the usual WS form with a radius $r_V = 1.25$ fm, diffuseness $a_V = 0.65$ fm, and a real potential depth $V_0 = 36.54$ MeV, which reproduces the binding energy ($E_b = 6.257$ MeV) of the $d + n$ structure of triton.

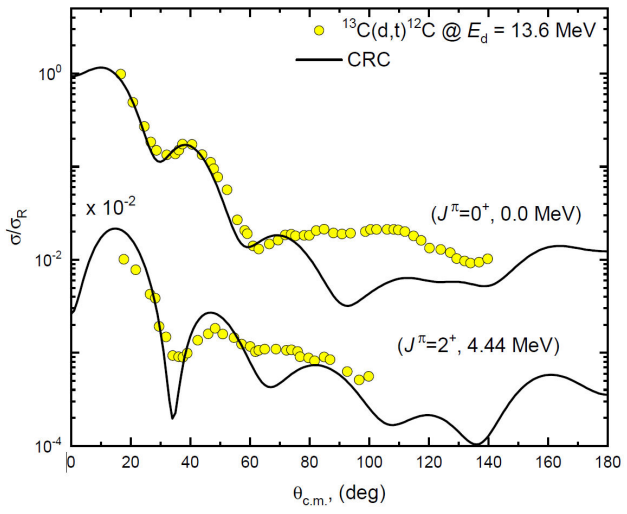

FIGURE 4. Experimental ADs for ^{13}C(d,t)^{12}C reaction at $E_d = 13.6$ MeV with the transition to the (0^+, 0.0 MeV) and (2^+, 4.43 MeV) ^{12}C states (solid circles) versus the CRC calculations (solid curves).

3.3. ^{13}C(d,n)^{14}N proton stripping transfer reaction

To examine the coupling effects of the (d,n) proton transfer reaction on the d+^{13}C elastic scattering channel, the previously measured AD for the ^{13}C(d,n)^{14}N reaction at E$_d$= 15.7 MeV leading to the ^{14}N ground state [15] is investigated within the framework of the CRC method. For the (d+^{13}C) channel, the generated with renormalizations N_{Reff}= 0.914 and N_{Ieff}= 0.576 was utilized. For the (n+^{14}N) channel at appropriate energy, the global CH89 [18] potential was employed. These potentials are given in Table I.

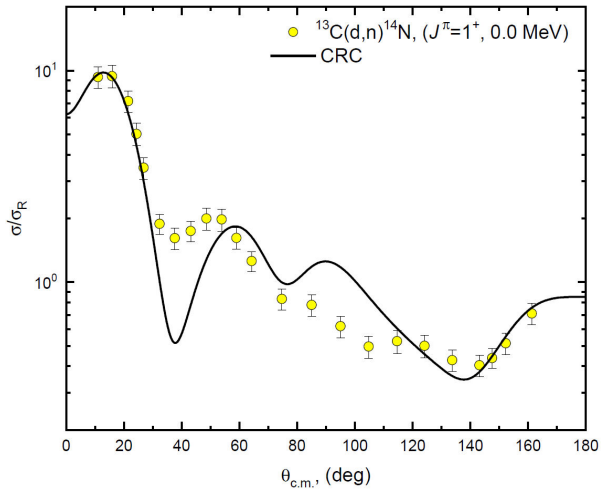

FIGURE 5. Experimental ADs for ^{13}C(d,n)^{14}N reaction at E$_d$= 15.7 MeV with the transition to the (1$^+$, 0.0 MeV) ^{14}N ground state (solid circles) versus the CRC calculation (solid curve).

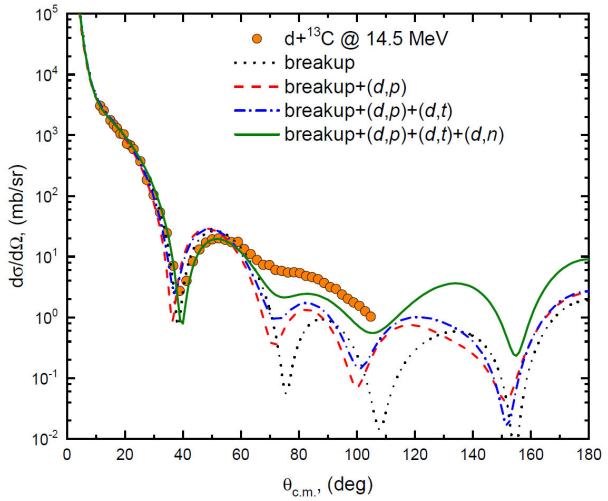

FIGURE 6. The d+^{13}C elastic AD at E$_d$= 14.5 MeV versus the calculations utilizing CDCC and CDCC+CRC methods. The dotted curve represents the breakup effect, the dashed curve includes breakup+(d,p), the dash-dotted curve includes breakup+(d,p)+(d,t), and the solid curve represents breakup+(d,p)+(d,t)+(d,n). These calculations were performed using a non-normalized $U_{\rm eff}$ (with N_{Reff} and N_{Ieff} fixed to unity).

The comparison between the experimental AD for the ^{13}C(d,n)^{14}N transfer reaction leading to the ^{14}N ground state at E$_d$= 15.7 MeV and the CRC calculations is reasonably good, as illustrated in Fig. 5. The optimal SAs for the two probabilities ($1P_{1/2}$ and $1P_{3/2}$) of the ^{14}N(1$^+$, 0.0 MeV)→ ^{13}C + p configuration were obtained by fitting the measured data over the full angular range, minimizing the χ^2/N. These values overestimate the previously calculated values [30], as shown in Table II.

To observe the different coupling effects on the d+^{13}C elastic scattering channel, we first studied the coupling effects coming from the (d,p) reaction, then from both the (d,p) and (d,t) transfer reactions, and finally the effects simultaneously come from the (d,p), (d,t), and (d,n) transfer reactions. These calculations were performed using the potentials parameters listed in Table I and the overlaps illustrated in Table II. In all these calculations, the previously generated $U_{\rm eff}$ from the CDCC calculations, without any adjustments (*i.e.*,) $N_{\rm Reff}$ and $N_{\rm Ieff}$ are fixed to unity), was employed for the d+^{13}C entrance channel. As shown in Fig. 6, the calculations highlight the significant coupling effects arising from the (d,p) and (d,n) transfer reactions on the elastic d+^{13}C AD, compared to the coupling effect from the (d,t) transfer reaction. The analyses confirm the importance of considering nucleon pickup and striping transfer mechanisms, in addition to breakup, when investigating systems involving deuterons. Clearly, the effect of these couplings is especially important at larger angles, greater than 60°. A similar conclusion was reached in several previous studies [7, 8, 10].

4. Summary

The quite recently measured d+^{13}C elastic scattering AD data at E_d = 14.5 MeV is analyzed within the framework of the CDCC method to investigate the deuteron breakup effect, as well as by the CDCC and CRC methods to assess the impacts of nucleon transfer and deuteron breakup on the considered system. For this purpose, several data sets, including ^{13}C(d,p)^{14}C, ^{13}C(d,t)^{12}C, and ^{13}C(d,n)^{14}N neutron/proton transfer reactions, were analyzed individually within the CRC method, and then all these transfer reactions were elucidated using the CDCC and CRC methods. The calculations showed that coupling effects arising from both the breakup and transfer reactions, (d,p) and (d,n), have a significant influence on the elastic channel. The observed less significant coupling effect from the (d,t) reaction on the d+^{13}C system is probably linked to the relatively small spectroscopic amplitudes, which are a result of the structure of ^{13}C. The $U_{\rm eff}$ potential, which is the sum of CF potential and DPP, extracted from the CDCC calculations for d+^{13}C system, was employed in the CRC calculations for the ^{13}C(d,p)^{14}C at E$_d$ = 15.3 MeV, leading to the (J^{π}= 0$^+$, 0.0 MeV), (J^{π}= 1$^-$, 6.09 MeV), and (J^{π}= 3$^-$, 6.73 MeV) states of ^{14}C, the ^{13}C(d,t)^{12}C transfer reaction at E$_d$ = 13.6 MeV, leading to the (J^{π}= 0$^+$, 0.0 MeV) and (J^{π}= 2$^+$, 4.43 MeV) states of ^{12}C, as well as the ^{13}C(d,n)^{14}N transfer reaction at E_d = 15.7 MeV, leading to the ground state of ^{14}N. Spectroscopic amplitudes for the following configurations: ^{14}C(0$^+$, 0.0)→ ^{13}C + n, ^{14}C*(1$^-$, 6.09 MeV)→ ^{13}C + n, ^{14}C*(3$^-$, 6.73 MeV)→ ^{13}C+n, ^{13}C→ ^{12}C(0$^+$, 0.0 MeV)+n, ^{13}C→ ^{12}C*(2$^+$, 4.43 MeV) + n, and ^{14}N→ ^{13}C+p were extracted and compared to those in literature.

Acknowledgments

This research was funded by the Committee of Science of the Ministry of Science and Higher Education of the Republic of Kazakhstan (Grant No. AP14972391 and Grant No. BR24992891).

1. G. H. Rawitscher, Effect of deuteron breakup on elastic deuteron-nucleus scattering, *Phys. Rev. C* **9** (1974) 2210, https://doi.org/10.1103/PhysRevC.9.2210
2. M. Yahiro *et al.*, Chapter III. Effects of Deuteron Virtual Breakup on Deuteron Elastic and Inelastic Scattering, *Prog. Theor. Phys. Supp.* **89** (1986) 32, https://doi.org/10.1143/PTPS.89.32.
3. N. Austern *et al.*, Continuum-discretized coupled-channels calculations for three-body models of deuteron-nucleus reactions, *Phys. Rep.* **154** (1987) 125, https://doi.org/10.1016/0370-1573(87)90094-9.
4. C. W. Johnson *et al.*, White paper: from bound states to the continuum, *J. Phys. G* **47** (2020) 123001, https://doi.org/10.1088/1361-6471/abb129.
5. P. Chau Huu-Tai, Systematic study of elastic and reaction cross sections of deuteron induced reactions within the CDCC approach, *Nucl. Phys. A* **773** (2006) 56, https://doi.org/10.1016/j.nuclphysa.2006.04.006.
6. N. Keeley, N. Alamanos, V. Lapoux, Comprehensive analysis method for (d,p) stripping reactions, *Phys. Rev. C* **69** (2004) 064604, https://doi.org/10.1103/PhysRevC.69.064604.
7. N. Keeley, R.S. Mackintosh, Pickup coupling effects in deuteron scattering: The case of d+^{40}Ca, *Phys. Rev. C* **77** (2008) 054603, https://doi.org/10.1103/PhysRevC.77.054603.
8. N. J. Upadhyay, A. Deltuva, F. M. Nunes, Testing the continuum-discretized coupled channels method for deuteron-induced reactions, *Phys. Rev. C* **85** (2012) 054621, https://doi.org/10.1103/PhysRevC.85.054621.
9. R. S. Mackintosh, N. Keeley, Strong pickup-channel coupling effects in proton scattering: The case of p+^{10}Be, *Phys. Rev. C* **76** (2007) 024601, https://doi.org/10.1103/PhysRevC.76.024601.
10. M. Kawai, M. Kamimura, K. Takesako, Chapter V. Coupled-Channels Variational Method for Nuclear Breakup and Rearrangement Processes, *Prog. Theor. Phys. Supp.* **89** (1986) 118, https://doi.org/10.1143/PTPS.89.118.
11. A. Amar, K. Rusek, Sh. Hamada, Effects of deuteron breakup and nucleon-transfer reactions on d+^{11}B elastic scattering, *Eur. Phys. J. A* **59** (2023) 182, https://doi.org/10.1140/epja/s10050-023-01094-5.
12. B. A. Urazbekov *et al.*, Single-particle and cluster modes of ^{13}C excited states of 3.09, 8.86 and 9.89 MeV, *Int. J. Mod. Phys. E* **31** (2022) 2250031, https://doi.org/10.1142/S0218301322500318.
13. L. I. Galanina *et al.*, Study of the Mechanism of the ^{13}C(d,p)^{14}C Reaction at E$_d$= 15.3 MeV, *Phys. Atom. Nuclei* **81** (2018) 176, https://doi.org/10.1134/S1063778818020084.
14. N. I. Zaika *et al.*, *Bull. Russian Academy of Sciences* **37** (1974) 140.
15. M. Febbraro *et al.*, (d,n) proton-transfer reactions on ^{9}Be, ^{11}B, ^{13}C, ^{14,15}N and ^{19}F and spectroscopic factors at E$_d$= 16 MeV, *Phys. Rev. C* **96** (2017) 024613, https://doi.org/10.1103/PhysRevC.96.024613.
16. I. J. Thompson, Coupled reaction channels calculations in nuclear physics, *Comput. Phys. Rep.* **7** (1988) 167, https://doi.org/10.1016/0167-7977(88)90005-6.
17. W. Alharbi, A. A. Ibraheem, Sh. Hamada, New microscopic analysis for ^{15}N(d,p)^{16}N neutron transfer reaction at 15 MeV, *Int. J. Mod. Phys. E* **32** (2023) 2350029, https://doi.org/10.1142/S0218301323500295.
18. R. L. Varner *et al.*, A global nucleon optical model potential, *Phys. Rep.* **201** (1991) 57, https://doi.org/10.1016/0370-1573(91)90039-O.
19. A. J. Koning and J.P. Delaroche, Local and global nucleon optical models from 1 keV to 200 MeV, *Nucl. Phys. A* **713** (2003) 231, https://doi.org/10.1016/S0375-9474(02)01321-0.
20. M. Lacombe, *et al.*, Parametrization of the Paris N-N potential, *Phys. Rev. C* **21** (1980) 861 , https://doi.org/10.1103/PhysRevC.21.861.
21. Y. Iseri, M. Yahiro and M. Kamimura, Chapter IV. Coupled-Channels Approach to Deuteron and 3He Breakup Reactions, *Prog. Theo. Phys. Suppl.* **89** (1986) 84, https://doi.org/10.1143/PTPS.89.84.
22. B. Mauyey *et al.*, Deuteron breakup effects on the d + ^{12}C, ^{15}N, ^{16}O, ^{24}Mg, ^{32}S, ^{58}Ni and ^{70}Ge elastic scattering angular distributions, *Chin. J. Phys.* **90** (2024) 155, https://doi.org/10.1016/j.cjph.2024.05.003.
23. P. Descouvemont, Four-body extension of the continuum-discretized coupled-channels method, *Phys. Rev. C* **97** (2018) 064607, https://doi.org/10.1103/PhysRevC.97.064607.
24. P. A. Schmelzbach *et al.*, Scattering of polarized tritons by 9Be and 12C, *Phys. Rev. C* **l7** (1978) 16, https://doi.org/10.1103/PhysRevC.17.16.
25. S. Yu. Mezhevych *et al.*, The ^{13}C+^{11}B elastic and inelastic scattering and isotopic effects in the ^{12,13}C+^{11}B scattering, *Nucl. Phys. A* **724** (2003) 29, https://doi.org/10.1016/S0375-9474(03)01478-7.
26. S. Yu. Mezhevych *et al.*, Excitation of ^{14}C by 45 MeV ^{11}B ions, *Nucl. Phys. A* **753** (2005) 13, https://doi.org/10.1016/j.nuclphysa.2005.02.119.
27. A. T. Rudchik, Yu.M. Tchuvilsky, Spectroscopic amplitudes of multinucleon clusters in 1p-shell nuclei and analysis of many-nucleon transfer reactions, *Ukr. Fiz. Zh.* **30** (1985) 819.
28. A. T. Rudchik *et al.*, The ^{11}B+^{12}C elastic and inelastic scattering at E(^{11}B) = 49 MeV and energy dependence of the ^{11}B+^{12}C interaction, *Nucl. Phys. A* **695** (2001) 51, https://doi.org/10.1016/S0375-9474(01)01106-X.
29. V. A. Ziman *et al.*, Channel couplings in the ^{12}C(^{14}N,X) reactions at E(^{14}N) = 116 MeV, *Nucl. Phys. A* **624** (1997) 459, https://doi.org/10.1016/S0375-9474(97)00328-X.
30. A. T. Rudchik *et al.*, Direct versus exchange processes in the reactions ^{7}Li(^{14}N, ^{14,15}N) at 110 MeV, *Nucl. Phys. A* **700** (2002) 25, https://doi.org/10.1016/S0375-9474(01)01319-7.